

Whole brain functional connectivity in clinically isolated syndrome without conventional brain MRI lesions

Yaou Liu^{1,2,3} · Zhengjia Dai^{4,5} · Yunyun Duan¹ · Jing Huang¹ · Zhuoqiong Ren¹ ·
Zheng Liu⁶ · Huiqing Dong⁶ · Ni Shu⁵ · Hugo Vrenken² · Mike P. Wattjes² ·
Frederik Barkhof² · Yong He⁵ · Kuncheng Li¹

Received: 14 August 2015 / Revised: 4 November 2015 / Accepted: 30 November 2015 / Published online: 29 December 2015
© European Society of Radiology 2015

Abstract

Objective To investigate brain functional connectivity (FC) alterations in patients with clinically isolated syndromes (CIS) presenting without conventional brain MRI lesions, and to identify the FC differences between the CIS patients who converted to multiple sclerosis (MS) and those not converted during a 5-year follow-up.

Methods We recruited 20 CIS patients without conventional brain lesions, 28 patients with MS and 28 healthy controls (HC). Normalized voxel-based functional connectivity strength (nFCS) was determined using resting-state fMRI (R-fMRI) and compared among groups. Furthermore, 5-years clinical follow-up of the CIS patients was performed to examine the differences in nFCS between converters and non-converters.

Results Compared to HC, CIS patients showed significantly decreased nFCS in the visual areas and increased nFCS in several brain regions predominately in the temporal lobes. MS patients revealed more widespread higher nFCS especially in deep grey matter (DGM), compared to CIS and HC. In

the four CIS patients converting to MS, significantly higher nFCS was found in right anterior cingulate gyrus (ACC) and fusiform gyrus (FG), compared to non-converted patients.

Conclusion We demonstrated both functional impairment and compensation in CIS by R-fMRI. nFCS alteration in ACC and FG seems to occur in CIS patients at risk of developing MS.

Key Points

- Both functional impairment and compensation occur in CIS without conventional brain lesions.
- MS patients revealed more widespread higher nFCS especially in deep grey matter.
- nFCS alteration may help stratifying CIS at risk of developing MS.

Keywords Multiple sclerosis · Clinically isolated syndrome · Resting-state fMRI · Functional connectivity strength · Deep grey matter

Yaou Liu and Zhengjia Dai contributed equally to this work.

✉ Yong He
yong.h.he@gmail.com

✉ Kuncheng Li
kunchengli55@gmail.com

Yaou Liu
asiaeurope80@gmail.com

¹ Department of Radiology, Xuanwu Hospital, Capital Medical University, Beijing 100053, People's Republic of China

² Department of Radiology and Nuclear Medicine, Neuroscience Campus Amsterdam, VU University Medical Center, Amsterdam 1007 MB, The Netherlands

³ Department of Neurology and Tianjin Neurological Institute, Tianjin Medical University, General Hospital, Tianjin 300052, People's Republic of China

⁴ Department of Psychology, Sun Yat-sen University, Guangzhou 510006, People's Republic of China

⁵ State Key Laboratory of Cognitive Neuroscience and Learning & IDG/McGovern Institute for Brain Research, Beijing Normal University, Beijing 100875, People's Republic of China

⁶ Department of Neurology, Xuanwu Hospital, Capital Medical University, Beijing 100053, People's Republic of China

Introduction

Multiple sclerosis (MS) is an inflammatory demyelinating disease of the central nervous system, and is the main cause of non-traumatic neurological disability in young adults [8]. Although the clinical course of MS is highly variable, the first manifestation of most MS is an acute or subacute episode of optic neuritis, a brain-stem/cerebellar syndrome or a spinal cord syndrome. This initial episode is known as a clinically isolated syndrome (CIS) [19, 22, 25]. Early diagnosis and treatment in high risk CIS is essential to prevent future axon pathology and slow the progression to definite MS [20]. The number and location of lesions in CIS patients have predictive value in terms of conversion and disability progression [18, 19]. However, it remains largely unknown as to whether functional changes in CIS patients without conventional brain MRI lesions might have potential value in predicting conversion to definite MS.

Resting-state fMRI (R-fMRI) is able to non-invasively measure spontaneous or intrinsic brain activity and has the potential value to detect early brain functional changes [10, 17]. To our knowledge, very few R-fMRI studies in CIS have been reported so far. Using the independent component analysis (ICA) method, Roosendaal et al. showed early synchronization changes in patients with CIS, which were not detectable anymore in those patients with relapsing remitting MS (RRMS) [30]. Using regional amplitude of low frequency fluctuation (ALFF) measurement, Liu et al. reported decreased baseline activity in several brain regions (e.g., precuneus and posterior cingulate cortex) in CIS patients [15], and increased activity mainly in thalamus in RRMS patients [16], implying transit functional changes in CIS replaced with more widespread cortical remapping processes. However, the ICA approaches can only detect abnormalities in brain connectivity associated with specific functional subnetworks and ALFF reflects resting-state neural activity amplitudes in brain regions. The whole brain functional connectivity (FC) pattern in CIS has not been examined. The functional connectivity strength (FCS) index [5, 35], which assesses the FC architecture of brain regions across the whole-brain by measuring the average Pearson correlation coefficients among all brain voxels, is closely associated with cerebral blood flow, aerobic glycolysis, and oxidative glucose metabolism [14, 33] and could be a sensitive measurement for detecting the functional changes in CIS.

Here, we used R-fMRI data to investigate the whole brain FC patterns in CIS without conventional brain MRI lesions, compared with RRMS and healthy controls (HC). Furthermore, we examined the FCS differences between the CIS-to-MS converters and non-converters based on 5-year clinical follow-up results.

Materials and methods

Participants

In this study, twenty patients presenting with CIS suggestive of MS [optic neuritis (ON), $n=13$; spinal cord syndromes, $n=7$; nine males and 11 females; mean age 32.8, SD 12.3], were prospectively examined within 6 months from onset. The CIS was diagnosed according to the following criteria [18, 19]: 1) a single clinical episode suggestive of MS without brain lesion on T2-weighted or fluid attenuated inversion recovery (FLAIR) images assessed by two experienced neuroradiologists (Y.L. and Y.D.); 2) exclusion of other possible diagnoses such as neuromyelitis optical spectrum diseases (NMOSD) or acute disseminated encephalomyelitis (ADEM); and 3) without image artefacts in structural and functional images. All CIS patients underwent clinical follow-up to confirm their conversion to clinically definite MS (CDMS) [26]. For comparison, we selected 28 relapsing-remitting MS (RRMS) patients (nine males and 19 females; mean age 34.6, SD 10.0) fulfilling the McDonald criteria [25] by matching them for age and gender to the CIS group. In addition, we selected 28 age- and sex-matched HC (ten males and 18 females; mean age 31.6, SD 11.4) with no previous history of neurological dysfunction and with normal findings on neurological examination. The main demographic and clinical characteristics of all the subjects studied are reported in Table 1. The subjects were all right-handed as measured by the Edinburgh Inventory [23]. The institutional review board of Xuanwu Hospital, Capital Medical University approved the study, and written informed consent was obtained from each participant.

Data acquisition

MRI was performed on a 1.5 T Siemens Sonata whole-body MR system in the Department of Radiology, Xuanwu Hospital, Capital Medical University. A standard head coil was used with foam padding to restrict head motion. The routine axial slices (including 2D T2-weighted and FLAIR images) were positioned parallel to the line that joins the AC-PC line, with in-plane resolution of $1 \times 1 \text{ mm}^2$, number of slices (30), and slice thickness (4 mm). Sagittal 3D T1-weighted magnetization-prepared rapid acquisition gradient echo (MPRAGE) (TR/TE=1970/3.9 ms, TI=1100 ms, flip angle (FA)= 15° , number of slices=176, slice thickness=1 mm, with in plane resolution of $1 \times 1 \text{ mm}^2$) images were also obtained. We used a gradient-echo echo-planar sequence sensitive to BOLD (Blood Oxygen Level Dependent) contrast to acquire functional images (TR/TE=2000/60 ms, FA= 90° , with in plane resolution of $1.875 \times 1.875 \text{ mm}^2$, acquisition time: 6.06 minutes). Twenty axial slices were collected with 5 mm thickness, and a 2 mm gap. During R-fMRI, subjects were

Table 1 Demographic and clinical characteristics ^a

| | MS | CIS | HC | p value |
|----------------------------------|--------------------------------------|-------------------------|------------------------|---------------------|
| N | 28 | 20 | 28 | / |
| Gender | 9 M/19 F | 9 M/11 F | 10 M/18 F | 0.43 ^b |
| Age (years) | 34.6±10.0 (18-55) | 32.8±12.3 (18-56) | 31.6±11.4 (18-56) | 0.55 ^c |
| EDSS | 2.7±1.4 (0-6) | 3.1±1.9 (1-7) | / | 0.40 ^d |
| Disease Duration (months) | 40.0±33.4 (7-10) | 2.9±1.6 (0.2-6) | / | <0.001 ^d |
| T2 Lesion Volume (ml) | 60.1±66.0 (0.8-252.1) | / | / | / |
| NBV(ml) | 1486±125 [#] (1228-1692) | 1537±117 (1289-1719) | 1577±92 (1404-1787) | 0.01 ^e |
| NGMV(ml) | 807±75 (631-942) | 822±79 (673-935) | 846±59 (729-964) | 0.12 ^e |
| NWMV(ml) | 680±56 [#] (566-791) | 714±48 (616-822) | 731±43 (675-840) | <0.001 ^e |

Abbreviations: CIS=clinically isolated syndrome; HC=healthy control; EDSS=Expanded Disability Status Scale; MS=multiple sclerosis; NBV=normalized brain volume; NGMV=normalized gray matter volume; NWMV=normalized white matter volume

^a Data are presented as mean±SD (range) except *N* and Gender.

^b Chi-square test.

^c Main effect of group in ANOVA.

^d Two-sample two-tailed t-test a.

^e Main group effect from ANCOVA using age and sex as covariates

[#] *p*<0.05 compared to HC, using Bonferroni test for post-hoc comparisons

instructed to keep their eyes closed, to remain motionless, and to not to think of anything in particular.

Brain lesion and brain volume analysis

Marking of T2 lesions and measurement of T2 lesion volume (T2LV) in MS patients was performed by an experienced neuroradiologist (Y.L.) with more than 8 years of experience by using MRIcro software (<http://www.mccauslandcenter.sc.edu/mricro/mricro/mricro.html>). Based on 3D MPRAGE, we obtained normalized brain volume (NBV), normalized gray matter volume (NGMV), normalized white matter volume (NWMV) for each subject by using SIENAX (Version 2.6; FMRIB Software Library, <http://www.fmrib.ox.ac.uk/fsl/>) [31].

R-fMRI analysis

Data preprocessing

Image preprocessing was carried out using Statistical Parametric Mapping <http://www.fil.ion.ucl.ac.uk/spm>) and Data Processing Assistant for Resting-State fMRI (DPARSF) [6]. For scanner stabilization and participants' adapting to the environment, the first five volumes were discarded. The remaining functional scans were first corrected for within-scan acquisition time differences between slices and further realigned

to the first volume to correct for interscan head motions. To minimize head movement artefacts, individuals with more than 3 mm of translation or 3 degrees of rotation in any direction were discarded. Next, the individual structural image (T1-weighted MPRAGE images) was co-registered to the mean functional image after motion correction using a linear transformation. The transformed structural images were then segmented into gray matter (GM), white matter, and cerebrospinal fluid by using a unified segmentation algorithm [2]. The motion-corrected functional volumes were spatially normalized to the Montreal Neurological Institute (MNI) space using the normalization parameters estimated during unified segmentation and then re-sampled to 3 mm isotropic voxels. After a linear trend of the time courses was removed, the band-pass filter (0.01-0.1 Hz) was applied to remove low-frequency drifts and high-frequency noise. Finally, six head motion parameters, mean global signal, white matter signal, and cerebrospinal fluid signal were extracted and regressed out from the data.

Whole-brain functional connectivity strength analysis

We performed whole-brain FCS analysis as follows. First, we computed the Pearson's correlations between the time series of all pairs of brain voxels and obtained a whole-brain FC matrix for each participant. The computation was constrained within a GM mask (*N*voxels=61,379) which was generated

by thresholding (a threshold of 0.2) on the mean GM probability map of all subjects. Then, for a given GM voxel, we computed its functional connectivity strength (FCS) using the following equation:

$$FCS(i) = \frac{1}{N-1} \sum_{j \neq i} z_{ij} \quad r_{ij} > r_0. \quad (1)$$

Where r_{ij} was the correlation coefficient between voxel i and voxel j , the r_{ij} was converted z_{ij} using Fisher Z-transformation, and r_0 was a threshold that was set to eliminate weak correlations possibly arising from signal noise ($r_0=0.2$ in this study). To minimize the influences of nuisance variables on inter-individual variation in FCS and make the FCS as a comparable scale between subjects, we further computed the normalized FCS (nFCS) for a given voxel, i , using the following equation:

$$nFCS(i) = \frac{FCS(i) - \overline{FCS}}{\sigma(FCS)}. \quad (2)$$

Where \overline{FCS} is the mean FCS across all the voxels in the GM mask, and $\sigma(FCS)$ is the standard deviation of the FCS in the GM mask. Finally, we obtained an nFCS map for each subject.

Statistical analysis

Group differences in demographic variables and brain volumes

Demographic and brain volumetric analyses were performed by using SPSS software (Version 18; SPSS, Chicago, Ill). Kolmogorov-Smirnov tests were performed together with visual inspection of histograms to assess normality of the variables. Comparisons of the demographic data and brain volume measurements between CIS, MS patients, and HC, and between converted and non-converted group of CIS were conducted using a general linear model (GLM), using age and sex as covariates. Bonferroni correction was applied to adjust for multiple testing when applicable.

Group differences in nFCS

Before statistical analysis of imaging data, all individual nFCS maps were spatially smoothed with a Gaussian kernel (full width at half-maximum = 4 mm). Statistical tests on the nFCS maps across groups (CIS, MS and HC) were performed using a voxel-based, one-way analysis of covariance (ANCOVA) with age, and gender as covariates followed by post hoc, two-sample t tests. Correction for multiple comparisons was performed by Monte Carlo simulations [13] using the AFNI AlphaSim program (<http://afni.nimh.nih.gov/pub/dist/doc/manual/AlphaSim.pdf>). A corrected significance level of 0.05 was obtained with a combined $p < 0.05$ and cluster size >

2295 mm³ for the ANCOVA analysis, and a combined $p < 0.05$ and cluster size > 486 mm³ for post hoc, two-sample t tests analysis (which was conducted within a mask showing group nFCS differences from the ANCOVA analysis).

Differences in nFCS between CIS converted to MS and non-converted

To examine the nFCS differences between CIS converters and non-converters, a voxel-wise general linear model (GLM) analysis was performed with age and gender as covariates. Multiple comparisons were corrected using Monte Carlo simulations. A corrected significance level of 0.05 was obtained with a combined $p < 0.05$ and cluster size > 486 mm³ for two-sample t tests analysis.

MRI-Clinical correlation

To determine the relationship between nFCS and clinical [Kurtzke Expanded Disability Status Scale (EDSS) and disease duration], and structural MRI variables (T2LV, NBWV, NGMV, NWMV), a voxel-based multiple linear regression analysis was separately conducted in the MS and CIS groups within regions showing significant nFCS differences in comparisons with the control group, considering age and gender as covariance. Multiple comparisons were corrected again using Monte Carlo simulations.

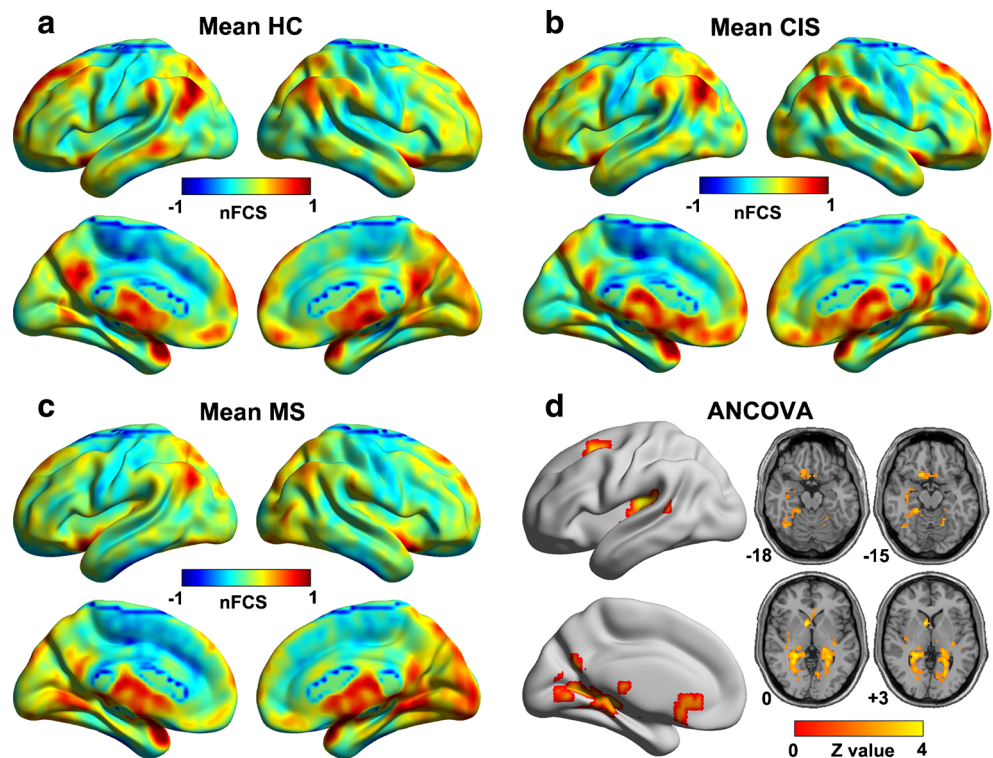
Results

Table 1 summarizes the clinical and demographic characteristics of the study participants. There were no group differences ($p > 0.1$) in age and gender among the different patient groups and HC. MS patients showed significant decreased NBV ($p = 0.01$) and NWMV ($p < 0.01$) compared to HC. There were no significant differences between MS and CIS, CIS and HC in any of the brain volume measurements including NBV, NGMV and NWMV ($p > 0.2$). After approximately 5 years (58.7 months, SD 6.6, range 43–68 months) in clinical follow-up, four of the 20 CIS patients (three myelitis and one ON) converted to CDMS.

nFCS difference among CIS, MS, and HC

There was no significant difference in the means [MS: 1587.2; CIS: 1519.7; HC: 1609.3. $F = 0.21$, $P = 0.813$] or standard deviations [MS: 574.0; CIS: 560.6; HC: SD 628.8. $F = 0.21$, $P = 0.814$] of FCS among three groups. The mean nFCS maps of each group are presented in Fig. 1. Visual examination indicated that the spatial distributions of brain regions with high nFCS were remarkably similar across the three groups in spite of some differences in strength. Those highly connected regions

Fig. 1 Within groups and statistical differences across groups in nFCS maps. Mean nFCS maps within the HC (a), CIS (b) and MS (c) groups indicate the spatial distributions of brain regions with high nFCS were remarkably similar across the three groups and the Z-statistical difference maps across groups (d) showed group differences in temporal regions, frontal regions, and thalamus (THAL). **Abbreviations:** ANCOVA, one-way analysis of covariance; CIS, clinically isolated syndrome; HC, healthy controls; MS, multiple sclerosis; nFCS, normalized functional connectivity strength



(i.e., higher nFCS) were primarily located in several parts of the default mode network (DMN) (mainly involving the bilateral medial frontal and parietal regions as well as lateral temporal and parietal regions), and occipital regions (Fig. 1 a, b, c). Further ANCOVA analysis revealed significant group differences in nFCS values mainly distributed in temporal regions [e.g., fusiform gyrus (FG), hippocampus (HIP), superior temporal gyrus (STG), Heschl's gyrus (HES), and insula (INS)], frontal regions [e.g., gyrus rectus (REC), middle frontal gyrus (MFG)], and thalamus (THA) (Fig. 1d).

Compared to the HC group, the CIS group showed significantly reduced nFCS values in four clusters, including the bilateral calcarine fissure and surrounding cortex (CAL), and left MFG, while increased nFCS was found in five clusters, including the bilateral olfactory gyrus, right FG, the posterior lobe of the cerebellum (PCL), and left rolandic operculum (ROL) (corrected $P < 0.05$) (Fig. 2a and Table 2). The MS group had significantly higher nFCS in several brain regions, especially in deep grey matter (DGM), such as THA, putamen (PUT), and caudate (CAU), compared to CIS and HC (corrected $P < 0.05$) (Fig. 2b, c and Table 2). Lower nFCS was only observed in the Left MFG and cuneus (CUN) in MS compared with HC (Fig. 2b and Table 2).

nFCS differences between CIS-to-MS converters and non-converters

In CIS patients, no significant difference of sex, age, EDSS, or brain volume measurements could be detected between

patients who developed CDMS and patients who did not ($p > 0.3$) (Table 3). The only significant difference in nFCS between these two groups was located in the right ACC and FG, which was significantly increased in the CIS group that developed CDMS (Fig. 2d). Moreover, the results between the two groups remained after taking the presenting symptoms as covariates.

Relationships between nFCS, clinical, and structural MRI variables

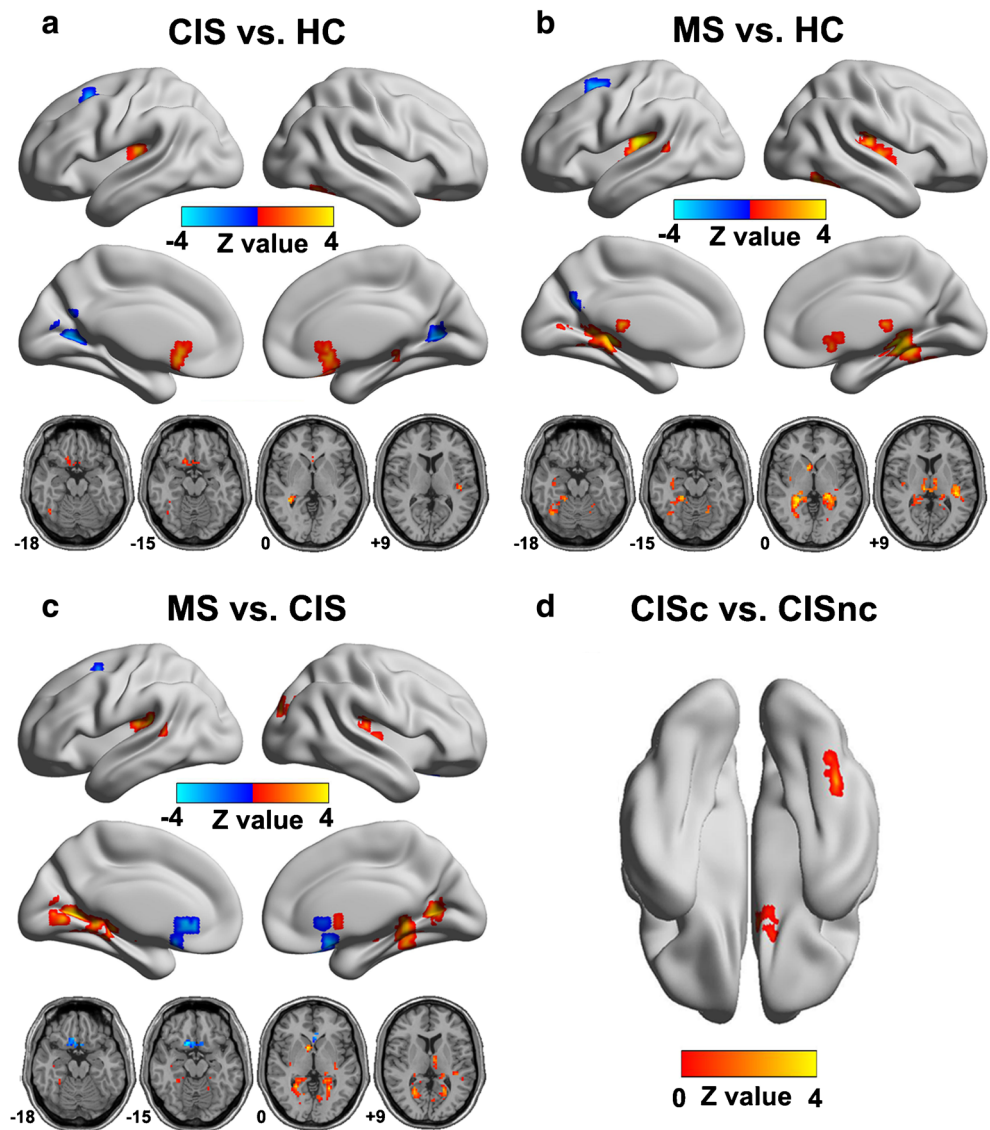
In the MS patient group, we observed significant positive correlations between the T2LV and regional nFCS values in the right FG, left HES, and left Hip and significant positive correlations between the EDSS and nFCS in the right Hip and FG ($P < 0.05$, corrected) (Fig. 3). No significant correlations between nFCS and brain volume measurements were identified in MS. Furthermore, we did not find any significant association between nFCS, brain volume measurements, and clinical variables in CIS.

Discussion

Alterations in resting-state brain activity can be observed in MS [16, 24, 28, 30]. However little is known about the whole brain FC changes at resting-state in CIS [15, 30, 34], especially CIS without focal brain MRI lesions. In the current study, we found both decreased and increased nFCS in CIS without

Fig. 2 Between-group nFCS maps. CIS patients showed nFCS changes in several brain areas of the occipital, temporary, and frontal lobes (a). MS patients demonstrated altered nFCS in several areas, especially in deep grey matter, compared to HC (b) and CIS (c). **d** Demonstrates difference of nFCS in right anterior cingulate cortex (ACC) and fusiform gyrus (FG) between CIS patients who converted to CDMS (CISc) and those not converted (CISnc).

Abbreviations: HC, healthy controls; CIS, clinically isolated syndrome; MS, multiple sclerosis; nFCS, normalized functional connectivity strength



brain lesions and demonstrated differences in nFCS between CIS and MS mainly in DGM by utilizing R-fMRI and voxel-based nFCS mapping. Furthermore, nFCS alteration in ACC and FG were identified in CIS patients that converted to MS at 5-year follow-up, compared to non-converters.

Both brain areas with decreased and with increased nFCS were found in CIS, implying that functional impairment and reorganization coexist in CIS patients without brain lesions or brain atrophy. The reduction in nFCS mainly occurred in visual areas including CAL and CUN, probably reflecting the visual impairment in these patients, which could be secondary to altered visual system inputs, as more than half of our CIS group has ON as their CIS manifestation. Increased nFCS in CIS was observed predominantly in the temporal lobe, which appears to be involved in high-level visual processing of complex stimuli such as faces (FG) and scenes (PHG) [32] or strongly related with visual stimulation (INS) [3]. The

increased nFCS in these areas can be interpreted as a functional adaption and/or epiphenomena in the visual system, contrasting with the functional damage in the CUN and CAL. In addition, functional reorganization in CIS was not limited to visual-related areas. Increased nFCS was found in ITG, HIP, and ACC, suggesting more widespread brain functional changes in domains reflecting memory, cognition, affection, and language [1].

The main difference between MS and CIS was the increased nFCS in DGM in MS including thalamus, putamen, and caudate. DGM structures such as the thalamus have extensive afferent and efferent connections with the midbrain and the cerebral cortex [12]. The nFCS increase in the DGM in MS in the current study corresponds well to previous studies either in task-related fMRI [21] or R-fMRI studies [16], highlighting the role of DGM as a coordinator or circuit element for brain plasticity and functional remapping in MS,

Table 2 Regions showing nFCS differences among the three groups

| Brain regions | BA | Vol mm ³ | MNI coordinates, mm | | | Maximum Z |
|------------------|-------|------------------------|---------------------|-----|-----|--------------|
| | | | x | y | z | |
| CIS<HC | | | | | | |
| Left MFG | 6 | 1242 | -30 | 9 | 51 | -4.09 |
| Left CAL | 30 | 837 | -21 | -63 | 9 | -3.08 |
| Left CAL | 31 | 567 | -6 | -72 | 12 | -2.94 |
| Right CAL | N/A | 1404 | 18 | -66 | 6 | -2.92 |
| CIS>HC | | | | | | |
| Right FG | 37 | 702 | 42 | -60 | -21 | 2.83 |
| OLF | 25 | 2214 | 0 | 18 | -6 | 3.09 |
| Right PCL | N/A | 756 | 45 | -48 | -45 | 3.43 |
| Left ROL | 13/41 | 1242 | -42 | -21 | 12 | 4.20 |
| Right FG | N/A | 1296 | 36 | -42 | -3 | 4.93 |
| MS<HC | | | | | | |
| Left MFG | 6/8 | 1863 | -21 | 15 | 54 | -3.43 |
| Left CUN/PCu | 31 | 513 | -6 | -63 | 24 | -3.11 |
| MS>HC | | | | | | |
| Left CAL | 30 | 648 | -21 | -72 | 3 | 2.69 |
| THA | N/A | 2781 | 9 | -24 | 9 | 3.64 |
| Right CAU | 25 | 810 | 9 | 9 | 3 | 3.65 |
| Left PUT | N/A | 540 | -33 | -12 | -6 | 3.92 |
| Left Hip | 19 | 5535 | -21 | -33 | -3 | 4.11 |
| Right ROL | 13 | 1998 | 42 | -21 | 18 | 4.16 |
| Right FG/Hip | 30/36 | 14499 | 24 | -33 | -6 | 5.04 |
| Left STG/ROL | 13/41 | 4536 | -36 | -24 | 15 | 5.10 |
| MS<CIS | | | | | | |
| Left SFG | N/A | 783 | -21 | 6 | 54 | -3.55 |
| REC | 25/11 | 3159 | 12 | 24 | -21 | -3.50 |
| MS>CIS | | | | | | |
| Left PUT | N/A | 621 | -33 | -12 | -6 | 3.07 |
| Left THA | N/A | 1026 | -6 | -9 | 9 | 3.20 |
| Right Hip/PUT | N/A | 864 | 33 | -12 | -6 | 3.21 |
| Left STG | 41/13 | 2214 | -45 | -33 | 18 | 3.51 |
| Right ROL | 13 | 1053 | 45 | -21 | 18 | 3.62 |
| Right CAL | 30/18 | 7074 | 27 | -51 | 0 | 3.87 |
| Left CAL | 30 | 6291 | -24 | -54 | 0 | 4.03 |
| Right CAU | N/A | 621 | 9 | 9 | 0 | 4.36 |

x, y, z, coordinates of primary peak locations in the MNI space; Z statistical value of peak voxel showing nFCS differences between the MS subjects and healthy elders (negative values: MS<HC; positive values: MS>HC).

Abbreviations: BA, Brodmann's area; CAU, caudate; CAL, calcarine fissure and surrounding cortex; CUN/PCu, cuneus/precuneus; FG, fusiform gyrus; Hip, hippocampus; ITG, inferior temporal gyrus; MFG, middle frontal gyrus; OLF, olfactory; PCL, posterior lobe of cerebellum; PUT, putamen; REC, rectus; ROL, rolandic operculum; SFG, superior frontal gyrus; STG, superior temporal gyrus; THA, thalamus; N/A, not applicable; nFCS, normalized functional connectivity strength. $P<0.05$, corrected for multiple comparisons.

compensating for the relative loss of cortex and gradual loss of afferent and efferent cortical connections. The relatively preserved function of the DGM in CIS suggests that DGM function can remain normal when structural damage remains mild. Furthermore, our functional MRI findings are consistent with the structural MRI observations that regional GM atrophy mainly confined to the DGM and not to cortical regions developed from clinical onset to conversion to MS [4]. This finding implies a temporal evolution of whole brain FC alterations especially in DGM during the disease progression which confirmed our previous study using the ALFF measure in a different patient cohort [16].

Comparing CIS patients who converted to MS with those not converting to CDMS at 5-year follow-up, there were no significant differences in demographic variables (such as age, sex, or EDSS) or brain volume measurements. The only significant difference was identified in nFCS, which was located in the right ACC and FG. The ACC plays a central role in a wide spectrum of highly integrated tasks, including visuo-spatial imagery, episodic memory retrieval, and self-processing operations [7] and is a key component of the DMN[27], which is defined by strong interactions between the PCC/precuneus and the inferior parietal lobule (IPL) and medial prefrontal cortex. Decreased activity of ACC was observed in progressive MS and more pronounced in cognitively impaired patients at resting-state in ICA [29]. Furthermore the FG is involved in high-level visual processing. Taken together, the increase of OLF/ACC and fusiform in CIS may imply a decrease in the brain reserve in brain functions, such as visual and cognitive systems, which give important clues to conversion to MS. Some previous studies also demonstrated decreased functional connectivity or ALFF in ACC in MS [29] and CIS patients [15]; the discordance with the current study may due to different analysis methods or different patient characteristics (such as disease subtypes, disease duration or EDSS). Further multi-centre studies with standardized analysis protocols would help clarify this discrepancy.

For MS patients, nFCS in several brain regions such as FG correlated with T2LV, suggesting that lesions do impact the brain functional changes. The association between increased nFCS and worse disability indicates that increased neural synchronization cannot prevent developing disability in MS patients. There is no correlation between nFCS with clinical variables in CIS, which implies functional changes in CIS as a transit or temporary phenomena will evolve as time passes after the initial presentation.

There are some methodology issues and limitations in this study. Firstly, this is a pilot study with a relatively small sample, which prevents us creating an R-fMRI model to predict the CIS conversion. Secondly, the rs-fMRI data were collected at a 1.5 T MRI with a 5 mm slice thickness (anisotropic resolution) and a 2 mm gap, which may leave some small brain regions not sampled; a high resolution fMRI study at 3.0 T is

Table 3 Comparison of clinical and brain volume measurements between converted group and non-converted groups after a 5-year clinical follow-up

| <i>N</i> | Non-converted group <i>N</i> =16 16 | Converted group <i>N</i> =4 4 | <i>p</i> value / |
|----------------------------------|---|-------------------------------------|---------------------|
| Gender | 9/7 | 1/3 | 0.26 ^a |
| Age (years) | 35.3±12.6 (19-56) | 26.0±9.4 (18-41) | 0.12 ^b |
| EDSS | 3.1±2.1 (1-7) | 3.3±1.6 (2-6) | 0.16 ^b |
| Disease Duration (months) | 2.5±1.8 (0.5-4.0) | 2.3±1.5 (0.2-6.0) | 0.79 ^b |
| NBV(ml) | 1544±125 (1289-1719) | 1515±97 (1383-1607) | 0.65 ^b |
| NGMV(ml) | 827±80 (673-935) | 810±84 (685-883) | 0.69 ^b |
| NWMV(ml) | 717±54 (616-822) | 705±17 (682-724) | 0.65 ^b |

Abbreviations: EDSS=Expanded Disability Status Scale; NBV=normalized brain volume; NGMV=normalized gray matter volume; NWMV=normalized white matter volume

Data are presented as mean±SD (range) except gender.

^a Chi-square test.

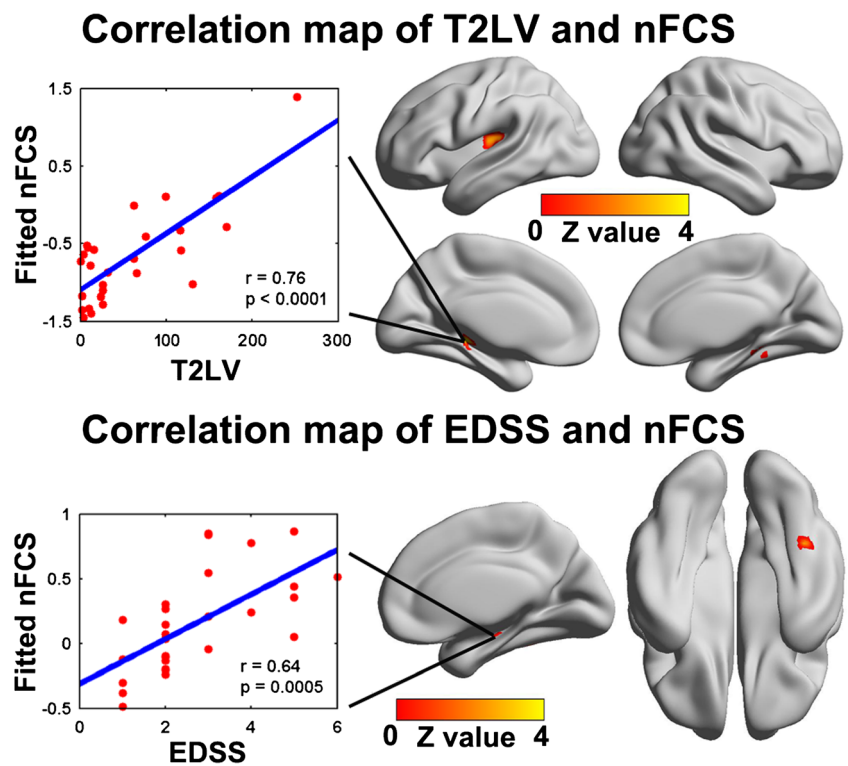
^b Two-sample two-tailed t-test.

required to confirm the current findings. Thirdly, we utilized the voxel-wise approach in the current study, which allows for the model-free examination of inter-voxel connectivity and, therefore, resulting in useful information on network organization [11] and avoids parcellation-dependent effects on network topology of the human brain networks. Combination

with ROI-based analysis is warranted to validate the current findings. Fourthly, as all the CIS patients without brain lesions were defined using conventional MRI, we cannot exclude the presence of cortical lesions in our CIS patients, which need further studies incorporating sequences such as double inversion recovery (DIR) [9] for demonstrating cortical lesions.

Fig. 3 Relationship of T2LV, EDSS and nFCS in MS. The upper panel shows correlation maps of T2LV and nFCS values in the right fusiform (FG), left Heschl’s gyrus (HES), and left hippocampus (Hip). The lower panel shows correlation maps of EDSS score and nFCS values in the right Hip and FG.

Abbreviations: EDSS, Kurtzke Expanded Disability Status Scale; MS, multiple sclerosis; nFCS, normalized functional connectivity strength; T2LV, T2 lesion volume



Finally, longitudinal R-fMRI examination would be important to see the dynamic functional changes from CIS to MS within patients, and confirm the predicted value of baseline activity.

In conclusion, we demonstrated both functional impairment and compensation in CIS without brain lesions using whole-brain voxel-based R-fMRI. A temporal evolution of nFCS changes from CIS to MS seems to occur especially in DGM. The nFCS alteration in ACC and FG may help stratifying CIS at risk of developing MS.

Acknowledgments The scientific guarantor of this publication is Yaou Liu. The authors of this manuscript declare no relationships with any companies, whose products or services may be related to the subject matter of the article. This work was supported by the ECTRIMS-MAGNMIS Fellowship from ECTRIMS (Y.L.), the National Science Foundation of China (Nos. 81101038, 81571631 and 30930029), the Beijing Natural Science fund (No.7133244), and the Beijing Nova Programme (xx2013045), the Beijing Municipal Administration of Hospitals Clinical Medicine Development of Special Funding Support (No.ZYLX201609). Dr. Hugo Vrenken has received funding from Novartis, Pfizer, and Merck Serono for collaborative research projects. Dr. Mike P. Wattjes serves as a consultant for Biogen, Novartis, and Roche. Prof. Frederik Barkhof serves as a consultant for Bayer-Schering Pharma, Sanofi-Aventis, Biogen Idec, Teva, Novartis, Roche, Synthon, and Jansen Research.

Dr. Yaou Liu, Dr. Zhengjia Dai, Dr. Yunyun Duan, Dr. Jing Huang, Dr. Zhuoqiong Ren, Dr. Zheng Liu, Dr. Huiqing Dong, Dr. Ni Shu, Professor Yong He, and Professor Kuncheng Li report no disclosures.

No complex statistical methods were necessary for this paper. Institutional Review Board approval was obtained. Written informed consent was obtained from all subjects (patients) in this study. Methodology: Prospective, diagnostic or prognostic study, performed at one institution.

References

- Allman JM, Hakeem A, Erwin JM, Nimchinsky E, Hof P (2001) The anterior cingulate cortex. The evolution of an interface between emotion and cognition. *Ann N Y Acad Sci* 935:107–117
- Ashburner J, Friston KJ (2005) Unified segmentation. *Neuroimage* 26:839–851
- Astafiev SV, Stanley CM, Shulman GL, Corbetta M (2004) Extrastriate body area in human occipital cortex responds to the performance of motor actions. *Nat Neurosci* 7:542–548
- Bergsland N, Horakova D, Dwyer MG et al (2012) Subcortical and cortical gray matter atrophy in a large sample of patients with clinically isolated syndrome and early relapsing-remitting multiple sclerosis. *AJNR Am J Neuroradiol* 33:1573–1578
- Buckner RL, Sepulcre J, Talukdar T et al (2009) Cortical hubs revealed by intrinsic functional connectivity: mapping, assessment of stability, and relation to Alzheimer's disease. *J Neurosci : Off J Soc Neurosci* 29:1860–1873
- Chao-Gan Y, Yu-Feng Z (2010) DPARSF: A MATLAB Toolbox for "Pipeline" Data Analysis of Resting-State fMRI. *Front Syst Neurosci* 4:13
- Christoff K, Ream JM, Geddes LP, Gabrieli JD (2003) Evaluating self-generated information: anterior prefrontal contributions to human cognition. *Behav Neurosci* 117:1161–1168
- Compston A, Coles A (2008) Multiple sclerosis. *Lancet* 372:1502–1517
- Geurts JJ, Pouwels PJ, Uitendaele BM, Polman CH, Barkhof F, Castelijns JA (2005) Intracortical lesions in multiple sclerosis: improved detection with 3D double inversion-recovery MR imaging. *Radiology* 236:254–260
- Gusnard DA, Raichle ME (2001) Searching for a baseline: functional imaging and the resting human brain. *Nat Rev Neurosci* 2:685–694
- Hayasaka S, Laurienti PJ (2010) Comparison of characteristics between region-and voxel-based network analyses in resting-state fMRI data. *NeuroImage* 50:499–508
- Herrero MT, Barcia C, Navarro JM (2002) Functional anatomy of thalamus and basal ganglia. *Childs Nerv Syst* 18:386–404
- Ledberg A, Akerman S, Roland PE (1998) Estimation of the probabilities of 3D clusters in functional brain images. *Neuroimage* 8:113–128
- Liang X, Zou Q, He Y, Yang Y (2013) Coupling of functional connectivity and regional cerebral blood flow reveals a physiological basis for network hubs of the human brain. *Proc Natl Acad Sci U S A* 110:1929–1934
- Liu Y, Duan Y, Liang P et al (2012) Baseline brain activity changes in patients with clinically isolated syndrome revealed by resting-state functional MRI. *Acta Radiol* 53:1073–1078
- Liu Y, Liang P, Duan Y et al (2011) Brain plasticity in relapsing-remitting multiple sclerosis: evidence from resting-state fMRI. *J Neurol Sci* 304:127–131
- Logothetis NK, Pauls J, Augath M, Trinath T, Oeltermann A (2001) Neurophysiological investigation of the basis of the fMRI signal. *Nature* 412:150–157
- Miller D, Barkhof F, Montalban X, Thompson A, Filippi M (2005) Clinically isolated syndromes suggestive of multiple sclerosis, part 2: non-conventional MRI, recovery processes, and management. *Lancet Neurol* 4:341–348
- Miller D, Barkhof F, Montalban X, Thompson A, Filippi M (2005) Clinically isolated syndromes suggestive of multiple sclerosis, part I: natural history, pathogenesis, diagnosis, and prognosis. *Lancet Neurol* 4:281–288
- Miller DH, Chard DT, Ciccarelli O (2012) Clinically isolated syndromes. *Lancet Neurol* 11:157–169
- Minagar A, Barnett MH, Benedict RH et al (2012) The thalamus and multiple sclerosis: modern views on pathologic, imaging, and clinical aspects. *Neurology* 80:210–219
- Noseworthy JH, Lucchinetti C, Rodriguez M, Weinshenker BG (2000) Multiple sclerosis. *N Engl J Med* 343:938–952
- Oldfield RC (1971) The assessment and analysis of handedness: the Edinburgh inventory. *Neuropsychologia* 9:97–113
- Pantano P, Petsas N, Tona F, Sbardella E (2015) The Role of fMRI to Assess Plasticity of the Motor System in MS. *Front Neurol* 6:55
- Polman CH, Reingold SC, Banwell B et al (2011) Diagnostic criteria for multiple sclerosis: 2010 revisions to the McDonald criteria. *Ann Neurol* 69:292–302
- Poser CM, Paty DW, Scheinberg L et al (1983) New diagnostic criteria for multiple sclerosis: guidelines for research protocols. *Ann Neurol* 13:227–231
- Raichle ME, MacLeod AM, Snyder AZ, Powers WJ, Gusnard DA, Shulman GL (2001) A default mode of brain function. *Proc Natl Acad Sci U S A* 98:676–682
- Rocca MA, Pagani E, Absinta M et al (2007) Altered functional and structural connectivities in patients with MS: a 3-T study. *Neurology* 69:2136–2145
- Rocca MA, Valsasina P, Absinta M et al (2010) Default-mode network dysfunction and cognitive impairment in progressive MS. *Neurology* 74:1252–1259
- Roosendaal SD, Schoonheim MM, Hulst HE et al (2010) Resting state networks change in clinically isolated syndrome. *Brain* 133:1612–1621
- Smith SM, Zhang Y, Jenkinson M et al (2002) Accurate, robust, and automated longitudinal and cross-sectional brain change analysis. *Neuroimage* 17:479–489

32. Squire LR, Stark CE, Clark RE (2004) The medial temporal lobe. *Annu Rev Neurosci* 27:279–306
33. Tomasi D, Wang GJ, Volkow ND (2013) Energetic cost of brain functional connectivity. *Proc Natl Acad Sci U S A* 110:13642–13647
34. Wu GF, Brier MR, Parks CA, Ances BM, Van Stavern GP (2015) An Eye on Brain Integrity: Acute Optic Neuritis Affects Resting State Functional Connectivity. *Invest Ophthalmol Vis Sci* 56:2541–2546
35. Zuo XN, Ehmke R, Mennes M et al (2012) Network centrality in the human functional connectome. *Cereb Cortex* 22:1862–1875